PHYSICAL REVIEW D VOLUME 13, NUMBER 7 1 APRIL 1976

Composite structure of hadrons and why data lie near an isospin bound*

N. A. Törnqvist†

Ames Laboratory—ERDA and Department of Physics, Iowa State University, Ames, Iowa 50011 and Research Institute for Theoretical Physics, University of Helsinki, Helsinki, Finland

(Received 24 November 1975)

The remarkable fact that nondiffractive scattering data tend to lie dangerously close to an isospin bound is discussed and it is shown how this phenomenon can be understood in models where the hadrons are composite. The isospin dependence is argued to be given by the interchange of low-momentum isospin-carrying constituents ("soft" quarks). The remaining constituents interact through strong ($I=0$ gluon) forces which do not depend on isospin. Because of the small momentum carried by the interchanged constituents, the isospin dependence factorizes approximately into a real function (or matrix when spin effects are taken into account) which depends on s and t. This function multiplies the isospin-independent gluon amplitude. There is a similarity between this factorization and the way in which radiative corrections, due to soft photons, factorize. In this framework saturation of an isospin bound can be understood as an approximate regularity of strong interactions.

I. INTRODUCTION

In reactions for which one can measure three or more charge channels (such as $\pi^+p\to\pi^+p$, $\pi^-p\to\pi^-p$, and $\pi^-p\to\pi^0n$) but which, through isospin invariance, are described by only two isospin channels, there are constraints and, in particular, inequalities which the data must satisfy. It is an increasingly puzzling regularity of nondiffractive scattering data that the data tend to lie dangerously close to such an isospin bound.

This regularity was pointed out for the first time in 1967–1968 for a very limited amount of data in[1] $\pi N\to K\Sigma$ and in[2] $\pi N\to\pi N$ at 180° between 0 and 600 MeV. As more and more data have become available it has spread to cover a much larger interval in energy and scattering angle[3,4] in $\pi N\to\pi N$ and $\pi N\to K\Sigma$ and is found also in other reactions[4] such as $KN\to KN$ at 180°, and possibly $\bar{K}N\to\pi\Sigma$, where the data are still incomplete or not sufficiently accurate to reach any clear conclusions.

There is no simple nonaccidental dynamical argument which can explain this phenomenon apart from a few special situations. Therefore, this regularity might provide an important clue toward a better understanding of strong interactions. In this paper we shall discuss one mechanism by which one can understand the phenomenon in models involving composite hadrons.

In terms of the amplitudes involved the phenomenon can be expressed as a reality condition on a bilinear form, which is invariant under rotations of the spin reference frame. For $\pi N\to\pi N$ this condition is

$$\mathrm{Im}(f_{1/2}f^*_{3/2}+g_{1/2}g^*_{3/2})\approx 0\,, \tag{1}$$

where f and g refer to the spin-nonflip and the spin-flip amplitudes, respectively, and the index refers to isospin. More precisely the smallness of (1) can be expressed in terms of a parameter B,

$$B=2\sqrt{2}\,\frac{\mathrm{Im}(f_{1/2}f^*_{3/2}+g_{1/2}g^*_{3/2})}{d\sigma_{1/2}/d\Omega+2d\sigma_{3/2}/d\Omega}\,, \tag{2}$$

which is bounded between -1 and $+1$. We refer to B as the isopolarization because of its algebraic similarity with the ordinary polarization.

Condition (1) written in terms of directly measurable quantities corresponds to the situation very near the isospin bound of Doncel, Michel, and Minneart (DMM),[5]

$$-\lambda\left(\frac{d\sigma_+}{d\Omega},\frac{d\sigma_-}{d\Omega},2\frac{d\sigma_{\rm ex}}{d\Omega}\right)-4K(s,t)\geq 0\,, \tag{3}$$

where $\lambda(x,y,z)=(x+y-z)^2-4xy$ and

$$\begin{aligned}K(s,t)&=\frac{1}{2}\frac{d\sigma_+}{d\Omega}\frac{d\sigma_-}{d\Omega}(1-\vec{\zeta}_+\cdot\vec{\zeta}_-)\\&=\frac{d\sigma_-}{d\Omega}\frac{d\sigma_{\rm ex}}{d\Omega}(1-\vec{\zeta}_-\cdot\vec{\zeta}_{\rm ex})\\&=\frac{d\sigma_{\rm ex}}{d\Omega}\frac{d\sigma_-}{d\Omega}(1-\vec{\zeta}_{\rm ex}\cdot\vec{\zeta}_-)\,,\end{aligned} \tag{4}$$

with the unit vectors $\vec{\zeta}_i$ as the spin rotation vectors defined from the polarization parameter P and spin rotation (R and A) parameters

$$\vec{\zeta}_i=(A_i,P_i,R_i)\,. \tag{5}$$

The indices $+$, $-$, and ex refer to the elastic π^+p, π^-p, and charge-exchange processes, respectively.

For 180° (and 0°) scattering g vanishes and condition (1) or (2) reduces to a condition of near phase degeneracy of the spin-nonflip amplitudes, whenever they are of comparable magnitude. The inequality (3) reduces [because $K(s,t)=0$] to the simple triangle inequality involving only cross sections

$$-\lambda\left(\frac{d\sigma_+}{d\Omega},\frac{d\sigma_-}{d\Omega},2\frac{d\sigma_{ex}}{d\Omega}\right)\geq 0\ , \qquad (6)$$

or equivalently

$$\frac{1}{2}\left[\left(\frac{d\sigma_+}{d\Omega}\right)^{1/2}-\left(\frac{d\sigma_-}{d\Omega}\right)^{1/2}\right]^2\leq\frac{d\sigma_{ex}}{d\Omega}\leq\frac{1}{2}\left[\left(\frac{d\sigma_+}{d\Omega}\right)^{1/2}+\left(\frac{d\sigma_-}{d\Omega}\right)^{1/2}\right]^2\ . \qquad (6')$$

The degeneracy condition $B=0$ corresponds at 180° to the situation with the triangle formed by the square roots of the cross sections (the charge-independence triangle) collapsing to a line.

At other angles the degeneracy condition $B=0$ also has an interesting geometrical interpretation.[4] The three spin rotation vectors $\vec{\zeta}^+$, $\vec{\zeta}^-$, and $\vec{\zeta}^{ex}$ define a tetrahedron. The volume of this tetrahedron is proportional to the square root of the left-hand side of Eq. (3). Thus when the inequality is saturated, or equivalently $B=0$, the tetrahedron collapses to a planar one.

Notice that the conditions above are invariant under rotations of the spin reference frame. With this invariance as a requirement, condition (1) is a unique generalization of the near phase degeneracy condition at 180°. This property singles out the DMM bound (3) from other isospin bounds studied in the literature.[6]

In the following we shall first (Sec. II) discuss certain special dynamical situations where the degeneracy condition (1) is satisfied, or equivalently the isospin bound (3) is trivially saturated. Section III is the main section of this paper, where we discuss how the observations can be understood more generally in models involving composite hadrons. In Sec. IV we point out a formal similarity between the factorization derived in Sec. III and the factorization of soft-photon corrections to scattering amplitudes. In Sec. V we recapitulate the most important results of the data analysis from Ref. 4. This section may be read after this Introduction, especially by those readers who are not familiar with the experimental evidence for the phenomenon we discuss. In the conclusions (Sec. VI) we summarize the most important points of this paper. In the Appendix we discuss our arguments of Sec. III in more detail using an infinite-momentum frame.

II. SPECIAL CASES WHERE CONDITION (1) FOLLOWS FROM SIMPLE ARGUMENTS

There are a few situations where the degeneracy condition (1) or (2) follows from simple dynamical arguments. These are not sufficient to explain the effects seen, except in limited kinematic regions, but they provide a good starting point for the discussion of our more general arguments in Sec. III.

(i) One isospin channel dominates. For example, in $\pi N\to\pi N$ at $T_{lab}=200$ MeV the $\Delta(1236)$ makes $f_{3/2}\gg f_{1/2}$; or in $\pi N\to K\Sigma$ at large s and small t the $I_t=\frac{1}{2}$ amplitude dominates over the exotic $I_t=\frac{3}{2}$ one. Condition (1) follows trivially, and in addition one has much stronger degeneracy conditions,

$$\alpha_1\frac{d\sigma_1}{d\Omega}=\alpha_2\frac{d\sigma_2}{d\Omega}=\alpha_3\frac{d\sigma_3}{d\Omega}\ , \qquad (7)$$

$$\vec{\zeta}_1=\vec{\zeta}_2=\vec{\zeta}_3\ . \qquad (8)$$

Here α_i are fixed numbers given by Clebsch-Gordan coefficients.

(ii) No isospin dependence exists. The s-channel isospin amplitudes are equal, and charge-exchange cross sections vanish. This can be considered as a special case of (i) with $I_t=0$ dominance. Pomeron exchange is an obvious example.

(iii) Exchange-degenerate Regge trajectories with equal signature factors (such as ρ-ω) predict equal t-channel isospin amplitudes. At large s and small t condition (1) as well as conditions (7) and (8) follow.

(iv) Very close to elastic-scattering threshold when no inelastic channels are open (as in $\pi N\to\pi N$ or $KN\to KN$ below 50 MeV) all amplitudes are nearly real. Therefore, the isopolarization (as well as the ordinary polarization) must be very small. The stronger degeneracy conditions (7) and (8) do not follow in this case.

(v) The effective interaction is very weak. Then, first-order diagrams are a good approximation to the full amplitudes. Since the first-order diagrams are real the full amplitudes are approximately real. As in case (iii) the isopolarization nearly vanishes [without (7) and (8) being satisfied]. As an example, we mention the constituent-interchange model (CIM) of Gunion, Brodsky, and Blankenbecler.[7]

These points suggest an approach toward an understanding of the phenomenon within a more general framework. It is natural to assume the strongest forces to have the largest symmetry and to be independent of isospin as in (ii) and (iii). The isospin-dependent interaction should be much weaker [cf. (v)]. However, this weaker interaction should have large effects on the scattering amplitudes and not only give rise to small additive corrections. The effect of the isospin-dependent interaction should appear in the amplitudes as a multiplicative factor. A simple way to obtain such a multiplicative isospin-dependent factor is to attribute the strong isospin-independent interaction and the weaker isospin-dependent interaction to different constituents of composite hadrons.

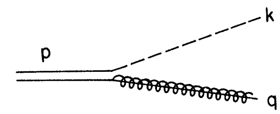

FIG. 1. The hadron bound state of two groups of constituents. The group of isospin-carrying soft constituents (ISC) is described by the dashed line. The remaining constituents (RC) are described by the curly and the solid lines.

III. THE ISOSPIN DEPENDENCE IN SCATTERING OF COMPOSITE HADRONS

A. A two-component picture of the hadron constituents

If one considers the hadrons as composite particles of confined constituents, it is clear that the isospin dependence of scattering amplitudes will be given by the dynamics of those constituents which carry isospin. In a quark-parton picture, the isospin-carrying constituents are the (valence) quarks, while the other constituents, i.e., the gluons and the possible sea of $q\bar{q}$ pairs, are isosinglets.

In order to simplify our discussion as well as to keep our arguments as general as possible, we divide the constituents into two groups:

(1) the isospin-carrying soft (low- but finite-momentum) constituents (ISC) (the soft quarks).

(2) the remaining constituents (RC) (the hard or high-momentum quarks, the gluons, and the $q\bar{q}$ pairs).

The dividing line between a soft and a hard constituent should (in order to motivate our approximations) be chosen such that the total energy and momentum carried by the first group of constituents is small, less than about 10% of the energy and momentum carried by the hadron. In the following we consider these two groups as if they were just two constituents.

In Fig. 1 we visualize the wave function describing the hadron as a bound state of the two groups of constituents. It will depend on the momenta, spins, and isospins involved. Omitting the spin index we denote it by

$$V = V(p, \vec{I}; k, \vec{I}^{\,\mathrm{ISC}}; q, \vec{I}^{\,\mathrm{RC}}) , \qquad (9)$$

where p, k, q denote the momenta and $\vec{I}, \vec{I}^{\,\mathrm{ISC}}, \vec{I}^{\,\mathrm{RC}}$ denote the isospins involved.

It is important to realize that these wave functions must be *real*. Ultimately this condition is due to unitarity and the condition that the constituents are confined. If Eq. (9) had an imaginary part, the latter would be proportional to the decay rate of the hadron to its constituents.

B. Intuitive picture of the nondiffractive collision

Imagine a classical bound system of a massive object surrounded by a slowly moving light object. Both objects can carry charge. If one neglects the small mass of the light objects the center of mass of the composite system coincides with that of the massive object. In a collision of the two systems at nonforward angles almost the entire momentum transfer must be transferred by the massive objects. The light objects interact weakly with each other, but can be rearranged in the collision. We assume that no charge can be exchanged in the over-all collision between the massive objects. Then any charge exchanged in the over-all collision must be exchanged by the light charge-carrying objects which have rearranged themselves. For a fixed scattering angle the probability for whether charge is exchanged or not will depend entirely on the rearrangement of the light objects. The rearrangement collision will, on the other hand, depend only on the nature of the bound states of the two constituents. We have here assumed that the time scale of the collision between the heavy objects is short compared to the other time scales involved.

C. The factorization of the isospin dependence

Let us now put this intuitive picture in somewhat more quantitative terms. We neglect initially all absorptive corrections. These may be large, but since the Pomeron is (predominantly) $I=0$ they cannot significantly change our results since all charge channels will be almost equally affected.

The hadronic amplitude can be described by the diagram of Fig. 2. Two interactions take place

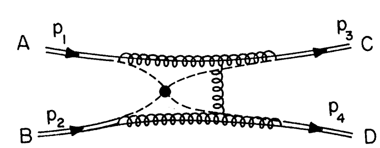

FIG. 2. A diagram visualizing hadron-hadron scattering. The curly line is the $I_t=0$ (gluon) interaction between the RC's.

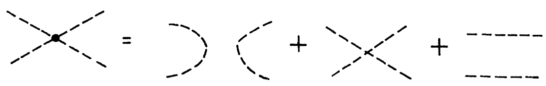

FIG. 3. The interaction between the ISC's as a rearrangement collision.

"simultaneously":

(i) a very strong isospin-independent interaction between the RC's,

(ii) a rearrangement of the ISC's. This means that we have assumed the interaction between the ISC's to be negligible compared to the other interactions involved. This second interaction can be visualized by the diagrams of Fig. 3. The ISC's behave as if they were free during the time of the very strong interaction (i). The interaction between the ISC's and the RC's appears only in determining the form of the bound-state wave-functions (9).

We can write the matrix element corresponding to Fig. 2 as

$$M(s,t,\ \text{isospin}) = \int \prod_{i=1}^{n}\left[\frac{d^4k_i}{(2\pi)^4} V(P_i,\vec{\text{I}}_i;k_i,\vec{\text{I}}_i^{\text{ISC}};q_i,\vec{\text{I}}^{\text{RC}})\right] \times R(k_1,\ldots,k_4;I_1^{\text{ISC}},\ldots,I_4^{\text{ISC}})C(q_1,\ldots,q_4)\delta(k_1+k_2-k_3-k_4). \qquad (10)$$

Here we have neglected spin effects; we return to these at the end of this section. The function R stands for the rearrangement collision and is a sum of products of δ functions (cf. Fig. 3). The interaction (i) is described by C, and does not depend on the isospins involved.

Now, the crucial result we shall need is that Eq. (10) should factorize into a product of two factors, one involving only R and the wave functions, the other involving only C (with or without the wave functions. The simplest and most natural way in which this can happen is related to our assumption that the ISC's carry a negligible momentum k_i. With this assumption factorization occurs provided C is smooth enough so we can replace its arguments $q_i = p_i - k_i$ by p_i. Then (10) factorizes into

$$M(s,t;\ \text{isospins}) = \tilde{R}(s,t;\ \text{isospins})C(s,t)\ , \qquad (11)$$

where

$$\tilde{R}(s,t;\ \text{isospins}) = \int \prod_{i=1}^{4}\left[\frac{d^4k_i}{(2\pi)^4} V(p_i,\vec{\text{I}}_i;k_i,\vec{\text{I}}_i^{\text{ISC}};q_i,\vec{\text{I}}^{\text{RC}})\right] R(k_1,\ldots,k_4;\vec{\text{I}}_1^{\text{ISC}},\ldots,\vec{\text{I}}_4^{\text{ISC}})\delta(k_1+k_2-k_3-k_4). \qquad (12)$$

In the Appendix we discuss this factorization in more detail using an infinite-momentum frame. The function R is a real function since it depends only on the real and nonsingular function V. The function C, on the other hand, is in general complex. Since C does not depend on isospin, the phases of all isospin amplitudes will be qiven by C. Thus within our approximations the phase-degeneracy condition or

$$\text{Im}[T(s,t,I_1)T^*(s,t,I_2)] \approx 0 \qquad (13)$$

follows. This condition is the analog of Eq. (1) for the spinless case or when only one spin amplitude is involved.

D. Spin complications

Let us now discuss the more general case with spin included. Obviously the spin dependence cannot factorize in the same way as the isospin (one would predict vanishing polarization), nor can (13) hold separately for every spin amplitude since it would then follow (if one requires the condition to be invariant under rotations of the spin reference frame) that all polarization (and spin rotation) data must be identical for all charge channels (e.g., $P^+ = P^-$) in clear contradiction to experiment. This means in our picture that both groups of constituents must carry spin and that both interactions depend on the spins involved. This is of course only what is to be expected for spin-carrying quarks and vector gluons.

We give below a simple heuristic derivation of the generalization (1) of Eq (13) when spin effects are included Let the spin dependence of the overall interaction be described by a matrix $T_{\mu\nu}$ with the index referring to the different spin configurations. For $0^-\frac{1}{2}^+ \to 0^-\frac{1}{2}^+$ scattering, T is given by the f and g amplitudes

$$T \propto \begin{pmatrix} f & g \\ -g^* & f^* \end{pmatrix} \qquad (14)$$

Condition (1) can be written

$$\text{Im}[\text{Tr}(T_{I_1}T_{I_2}^\dagger)] \approx 0. \qquad (15)$$

Now let us look at the diagram of Fig. 2 as two successive interactions occur. The first interaction describes the dissociation of the incoming hadron and the rearrangement of the ISC's. The second interaction describes the scattering of the RC's and the recombination into the outgoing hadrons. Let the spin dependence of the interactions be described by matrices R_I and C, respectively. Then the matrix T is the product of these two matrices, $T=R_IC$. Substituting this into (15) we get

$$\mathrm{Im}[\mathrm{Tr}(R_{I_1}CC^\dagger R_{I_2}^\dagger)]\approx 0. \tag{16}$$

The matrices R_{I_1} and R_{I_2} are real matrices since as in the spinless case they depend on the real wave functions. Since $CC^\dagger$ is obviously real, (16) is satisfied.

The generalization of (1) to processes involving many spin amplitudes is evidently

$$\mathrm{Im}\left(\sum_\lambda T_{I_1,\lambda}T^*_{I_2,\lambda}\right)\approx 0, \tag{17}$$

where the sum is over all spin amplitudes involved. Here the $T_{I\lambda}$'s stand for any n-particle amplitude from which diffraction has been removed, e.g., the three-particle process $\pi N\to\pi\pi N$, $KN\to K\pi N$, or $KN\to\pi\pi\Lambda$. To test the relation (17) directly with experimental data is very difficult It involves in principle (as in the $0^-\frac{1}{2}^+\to 0^-\frac{1}{2}^+$ case) almost complete measurements of the differential cross sections and spin rotation data for three charge channels. With the advent of phase-shift analysis for meson-production processes tests of (17) become feasible.

IV. COMPARISON WITH RADIATIVE CORRECTIONS DUE TO SOFT PHOTONS

The crucial step in the discussion of Sec. III was the factorization of the isospin dependence. We find it interesting that this factorization is similar to the factorization of soft-photon corrections.

The virtual-soft-photon corrections to a hadronic amplitude $AB\to CD$ is to second order in α given by diagrams such as Fig. 4. This gives a correction factor to the original amplitude T of the form[8]

$$T(s,t)=T_0(s,t)[1+\Delta(s,t)], \tag{18}$$

where

$$\Delta(s,t)=\tfrac{1}{2}\int_\lambda^\Lambda d^4q\,A(q,s,t), \tag{19}$$

with λ and Λ as the usual cutoffs and

$$A(q,s,t)=\frac{-i}{(2\pi)^4(q^2-i\epsilon)}\times\sum_{n,m}\frac{e_ne_m\eta_n\eta_m(p_n\cdot p_m)}{(p_n\cdot q-i\eta_n\epsilon)(-p_m\cdot q-i\eta_m\epsilon)}. \tag{20}$$

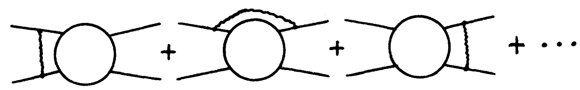

FIG. 4. Diagrams contributing to the virtual-soft-photon corrections to a hadronic amplitude $AB\to CD$ to second order in α.

Here q is the photon momentum, p_n the hadron momenta, e_n the hadron charges, and $\eta_n=+1$ or -1 for an incoming or outgoing line, respectively. One can take into account the higher-order soft-photon corrections by exponentiating the second-order correction

$$T(s,t)=T_0(s,t)e^{\Delta}(s,t). \tag{21}$$

The logarithmic divergence for $\lambda\to 0$ in (19) is canceled by adding the contributions from real emitted soft photons. We notice that the soft photon radiative corrections appear as a multiplicative correction factor for each s and t. The reason for this factorization is the fact that the soft photons carry a negligible momentum so that in any diagram involving soft photons, the momenta p_i in the purely hadronic part of the diagram are the same as in the over-all process.

Although the correction to the original amplitude as described by Eq. (21) is generally very small and the dynamics very different, the reason for the factorization is similar to the factorization discussed in Sec. III C. The soft photons correspond in this analogy to the isospin-carrying soft constituents. The analogy might have a deeper significance in theories attempting to unify strong and electromagnetic interactions.

V. COMPARISON WITH EXPERIMENTS

We shall here review the most important results from previous analyses of experimental data. For a detailed discussion of the method of analysis and for references to all the experimental papers we refer our readers to Ref. 4.

A. Backward $\pi N\to\pi N$ and $KN\to KN$ and forward $\pi N\to K\Sigma$ scattering

The analysis is simplest for 180° or 0° scattering [cf. Eq. (6)]. In Figs. 5, 6, and 7 the backward cross sections for $\pi^-p\to\pi^0n$, $K^+n\to K^0p$ and the K-meson forward cross sections for $\pi^-p\to K^+\Sigma^-$ are shown together with the isospin bounds. Figures 6 and 7 illustrate this behavior of the data by showing the fractional cross sections on the triangular isospin diagram.

As can be seen the data tend to lie close to the lower bound (or close to the circle in the isospin diagram). Of the total number of experimental

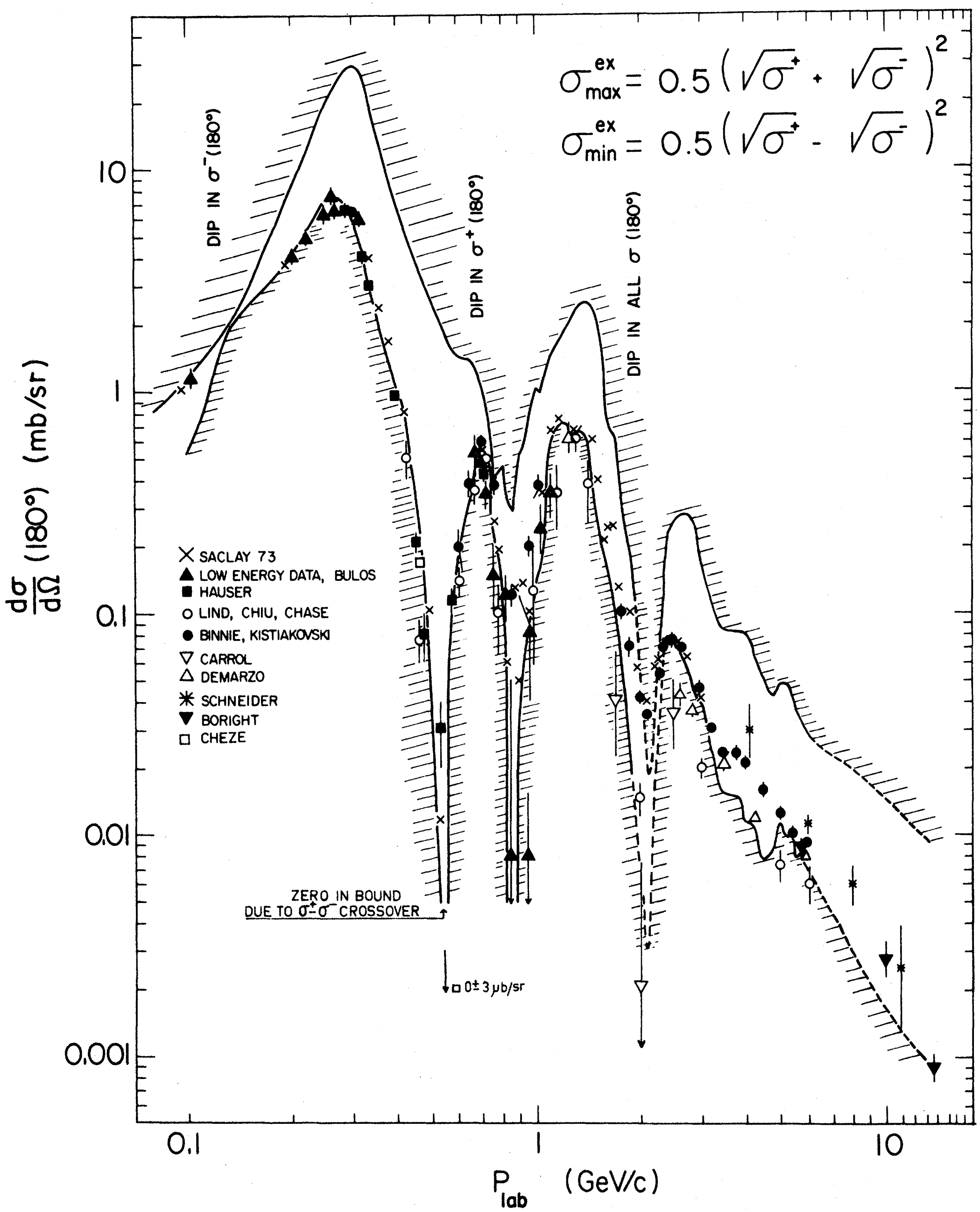

FIG. 5. The $\pi^- p \to \pi^0 n$ backward cross sections with the isospin bounds (6′). The crosses are Saclay phase-shift predictions.

points (which come from numerous different experiments) about half lie, in fact, slightly outside the bound. This is what should be expected on statistical grounds, if they really lie at the bound.

In the $K^+ n \to K^0 p$ phase-shift analyses (the curves C and D) there are difficulties fitting the data because of their nearness to the bound. In Figs. 5–7 the simple arguments of Sec. II apply only in a few comparatively narrow energy intervals such as those

very close to threshold in $\pi N \to \pi N$,

near 300 MeV/c and 1400 MeV/c in $\pi N \to \pi N$, where the $\Delta(1236)$ and $\Delta(1950)$ dominate,

at 740 MeV/c in $\pi N \to \pi N$, where the two bounds nearly coincide because of $I_s = \frac{1}{2}$ dominance,

above 3 GeV/c in $\pi N - K\Sigma$, where K^* exchange dominates.

Elsewhere the phenomenon is definitely nontriv-

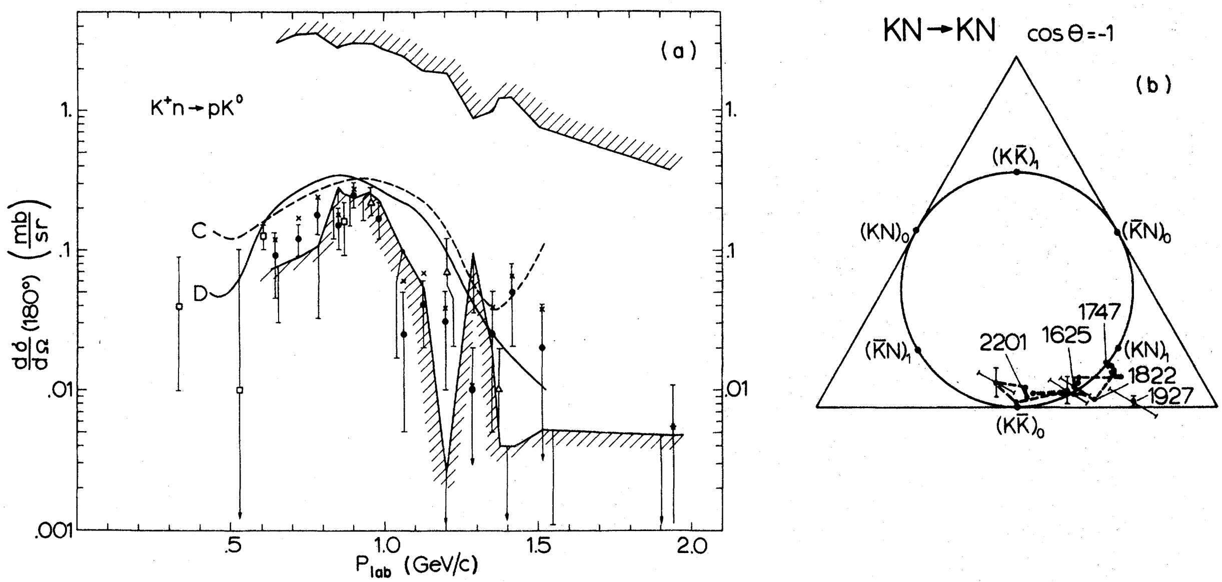

FIG. 6. The $K^+n\to K^0p$ backward cross sections with the isospin bounds. To the right are the same data plotted in an isospin diagram.

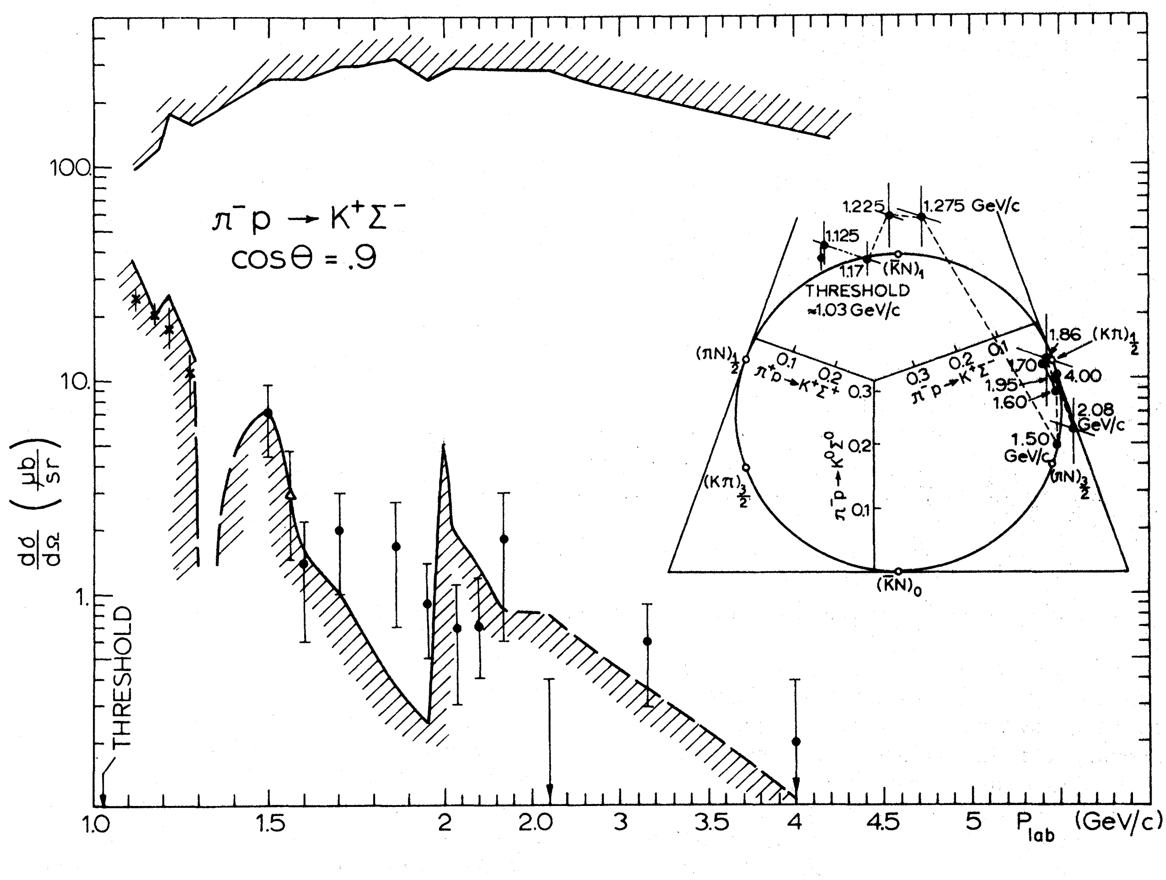

FIG. 7. The $\pi^-p\to K^+\Sigma$ data at $\theta_K=0°$ with the isospin bounds. Inserted is the corresponding isospin diagram with the same data.

ial. In particular notice that there is a zero in the lower bound of $\pi^- p - \pi^0 n$ near 550 MeV/c. Remarkably enough a recent experiment (Cheze *et al.*)[9] finds a charge-exchange cross section consistent with zero, 0.0 ± 0.3 mb.

In the region of the strong dip in all three cross sections of $\pi N \to \pi N$ near 2 GeV/c and in the energy region 2.5–6 GeV/c the situation is not clear owing to conflicting data. The most recent charge-exchange data (De Marzo *et al.*)[10] in the latter region lie quite near the lower bound.

In addition to these three reactions discussed above, it would be interesting to look at 180° $\bar{K}N \to \bar{K}N$, $\pi N \to K\Sigma$, and 0° and 180° $\bar{K}N \to \pi\Sigma$. Although there are some indications that the same phenomenon exists also in these reactions, the data are not yet sufficiently accurate to draw any clear conclusions.

B. Intermediate angles

At intermediate angles the analysis becomes considerably more complicated. To study the inequality (3) directly with data requires in addition to cross sections polarization and even some spin rotation data for all three charge channels. [It is possible to rewrite (3) so that it involves, up to a sign ambiguity, only cross-section and polarization data.[4]]

However, through phase-shift analyses the amplitudes are approximately known and we can study how well (1) is satisfied. Unfortunately, for small B, data are sensitive to B^2 [or, better, $(1-B^2)^{1/2}$] rather than B. Therefore, one cannot hope to get very sensitive tests of (1) with present uncertainties in the original data. In fact because of this effect values of B as large as 0.5 give as good a fit as does $B=0$ to the same data within typical experimental uncertainties. We hope this effect is partly compensated by the fact that phase-shift solutions should be more reliable than the raw data. In Fig. 8 we show a topographical plot in the $\cos\theta_{\text{c.m.}}$-p_{lab} plane of a quantity which measures how near the bound (3) the solution is. This quantity is essentially $B^2 \times \text{sign}(B)$. (For an exact definition see Ref. 4.) The thick solid curves correspond to lines where B changes sign, i.e., $B=0$, and the bound (3) is exactly saturated. Everywhere in the unshaded regions the solution lies near the bound, within typical experimental errors. The shaded regions correspond to situations where the data are one or more typical standard deviations from the bound One sees that apart from a few very small isolated and hardly significant regions the phenomenon at 180° extends as far out as to $\cos\theta \leq -0.1$ above $E_{\text{c.m.}} = 1.5$ GeV. For more forward angles, where diffraction contributes and our arguments of Sec. III do not apply, there are three

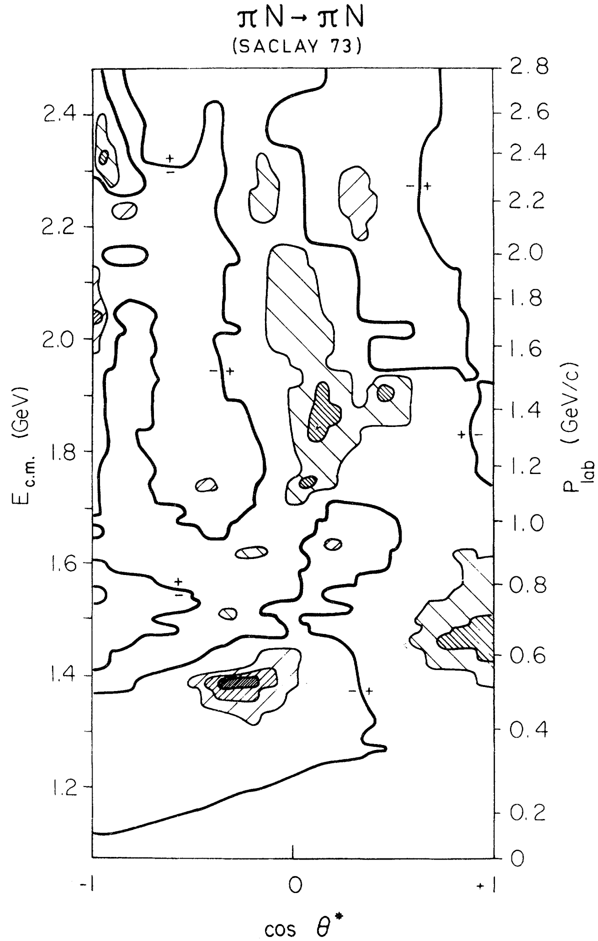

FIG. 8. Topographical map in the $\cos\theta$-P_{lab} plane of a quantity which measures the nearness of the data to the bound (3). The shaded regions correspond to regions where the data are more than approximately one typical standard deviation from the bound. The thick solid lines are zero lines of B or lines along which (3) is satisfied exactly as an equality. The graph is computed from the Saclay phase-shift analysis.

regions where one is definitely not close to the bound.

In $KN \to KN$ the situation is similar.[4] Different phase-shift solutions give rather different topographical plots, but they agree in that one is generally not more than one standard deviation from the bound for scattering angles in the backward hemisphere.

C. Statistical tests

The significance of the effects can be studied by comparing with a statistical model. In such a model one assumes random phases and random relative magnitudes of the amplitudes such that any "direction" in the space spanned by the complex vectors $(f_{1/2}, f_{3/2})$ and $(g_{1/2}, g_{3/2})$ is equally

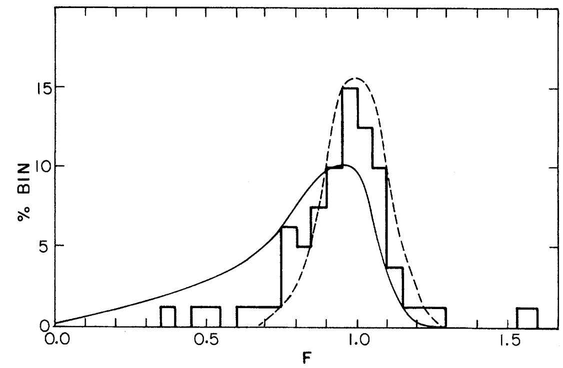

FIG. 9. Distribution of the backward $\pi N \to \pi N$ data in the variable $F=(1-B^2)^{1/2}$ (the radial distance in the isospin diagram). The solid curve is the prediction from the statistical model and the dashed curve is a Gaussian distribution around $F=1$ with variance $=0.1$.

probable. At 180° such a model predicts that all values of B should be equally probable; i.e., the distribution in the isopolarization B is uniform.

In Fig. 9 we show the distribution of the experimental 180° $\pi N \to \pi N$ points (same data as in Fig. 6) plotted versus the variable $F=(1-B^2)^{1/2}$. This variable has the advantage over B in that it is simply related to the data and that data violating the bound (6) have $F>1$ (F is the radial distance in the isospin diagram). As can be seen in Fig. 9 the data are peaked very much like the Gaussian dashed curve around $F=1$ with roughly equal numbers of points outside the bound $F>1$ as inside $F<1$. The variance of the peak is what is expected from typical 10–15% uncertainties in the data.

The solid curve in Fig. 9 corresponds to the prediction of the statistical model with a 10% experimental resolution folded in. In Ref. 4 other such comparisons with statistical models are done with the conclusion that in nondiffractive regions distributions in B agree better with the hypothesis $B\approx 0$ than with the random amplitudes generated by the statistical model. However, present experimental data are (owing to the geometrical effect discussed above) generally not accurate enough to put stronger limits on B than $B<0.5$.

VI. CONCLUDING REMARKS

We have argued that one can understand the approximate relations Eqs. (1) or (17) if the isospin dependence is given through the rearrangement of nearly free constituents which carry isospin but only a small fraction of the momentum. Most of the momentum transferred in the collision is mediated by neutral isosinglet constituents (gluons).

We believe that such a picture is compatible with most current models of composite hadrons. From lepton-proton experiments we know that approximately half of the proton momentum is carried by the quarks, while the rest is carried by neutral constituents. Furthermore, from the structure functions we know that the most probable momentum of a constituent is small. Thus if one assumes that the fastest quarks fly through, the remaining quarks must carry a small fraction of the total hadron momentum. Thus we believe our assumption that the rearranged quarks have small momentum is fairly general.

In order to achieve the factorization of the isospin dependence as discussed in Sec. III and in the Appendix the rearranged quarks must furthermore behave as if they were approximately free. This is in accordance with the usual assumption made in parton models.[11] However, according to the ideas of asymptotic freedom and infrared slavery the constituents with very small momenta should interact very strongly. Therefore, what we have called a soft- or low-momentum quark really should mean a "low- but not too low-" momentum quark (i.e., not a "wee" parton). This means that the rearranged quarks should not belong to the $q\bar{q}$ sea but to the valence quarks. While the $q\bar{q}$ sea is distributed like $1/x$ for small x, the valence quark distributions presumably do not grow so fast for small x, having additional factors $x^{1-\alpha}$ with $\alpha\approx\frac{1}{2}$. With the usual $(1-x)^n$ falloff for large x, the average valence quark's x is small but finite. A rearrangement of the quarks in the seas leads to only isospin-zero exchange, and it is usually attributed to Pomeron exchange, which we have assumed not to be present in the reactions studied.

As to a comparison with the CIM[7] a few comments are in order. If we remove the gluonic interaction described by C our model reduces essentially to the CIM for exclusive scattering. Therefore, the CIM also predicts that our relations (1) and (17) should be satisfied in the regions of large s, t, and u where the model is applicable. In addition it predicts vanishing polarization because all amplitudes are real. However, there is a great difference in the different approximations made in the two models. In the CIM the rearranged constituents carry a large fraction of the momenta and the asymptotic behavior of the wave functions for large k becomes important. In our case no wave function needs to absorb a large momentum since most of the momentum transfer is mediated through the gluonic amplitude C. However, since the amplitudes are very small at large angles it is quite possible that the two models are compatible with each other if the function C is chosen appropriately.

ACKNOWLEDGMENTS

We are very grateful to Professor Kenneth Lassila and W. J. Kernan, Jr., for useful comments and for their kind hospitality at Iowa State University, and to Professor Kenneth Lassila for a careful reading of the manuscript.

APPENDIX: THE AMPLITUDE EVALUATED IN AN INFINITE-MOMENTUM FRAME

Just as in the CIM[7] it is useful to discuss the amplitude of Fig. 2 or Eq. (10) in an infinite-momentum frame (IMF).[12] Thereby one achieves considerable simplification in the treatment of bound-state wave functions since graphs with backward moving lines vanish. This is of course only a technical simplification; it involves in itself no approximations.

We chose a particular IMF defined by

$$\begin{aligned} &\vec{p}_A = (\vec{p}_{C\perp} + \vec{p}_{D\perp}, P),\\ &\vec{p}_B = (\vec{0}_\perp, P),\\ &\vec{p}_C = (\vec{p}_{C\perp}, P),\\ &\vec{p}_D = (\vec{p}_D, P), \end{aligned} \tag{A1}$$

$$\vec{k}_i = (\vec{k}_{i\perp}, x_i P), \tag{A2}$$

$$q_i = p_i - k_i, \tag{A3}$$

$$p_i = (E_i, \vec{p}_i). \tag{A4}$$

The energies are fixed by the mass-shell conditions

$$p_i^2 = M_i^2, \tag{A5}$$

which are to order $1/P$ equal to P. This frame is the same as used, e.g., in Ref. 7 and has the advantage that the variables t and u (and s) are very simply related to the $\vec{p}_{C\perp}$ and $\vec{p}_{D\perp}$

$$\begin{aligned} t &= (p_A - p_C)^2 = -\vec{p}_{C\perp}^{\,2},\\ u &= (p_A - p_D)^2 = -\vec{p}_{D\perp}^{\,2}. \end{aligned} \tag{A6}$$

In the equal-mass case we have furthermore the orthogonality relation

$$\vec{p}_{C\perp} \cdot \vec{p}_{D\perp} = 0. \tag{A7}$$

In this case of equal masses the IMF chosen corresponds to a frame obtained when the laboratory frame is boosted orthogonally to the scattering plane such that the longitudinal momenta in the boost direction are P. This P is allowed to tend to infinity. The two-momenta $\vec{p}_{i\perp}$ still correspond to the external hadron momenta in the laboratory frame. These "transverse" momenta should thus not be confused with internal transverse momenta, which has a sharp falloff at a fixed small value. On the other hand, the variables x_i refer, of course, to the longitudinal fraction of the momentum in the boost direction, and should not be confused with x defined in, say, the laboratory or the c.m. frame. Using the rules of field theory in the IMF, we can write the amplitude as

$$M \propto \left[\frac{1}{(2\pi)^3}\right]^4 \int \prod_{i=1}^{4} \left[\frac{dx_i d^2\vec{k}_{i\perp}}{x_i(1-x_i)} V_i\right] C \cdot R (2\pi)^3 \delta(x_1 + x_2 - x_3 - x_4)\, \delta^2(\vec{k}_{1\perp} + \vec{k}_{2\perp} - \vec{k}_{3\perp} - \vec{k}_{4\perp}). \tag{A8}$$

[The irrelevant normalizations of V, C, and R are not the same here as in Eq. (10).] We shall mainly be interested in the factorization of R and C, and therefore we shall not limit the following discussion to R standing for a rearrangement collision. Thus C and R are arbitrary functions of $\vec{q}_i$ and $\vec{k}_i$, respectively. The function R is dependent on the isospin whereas C is not. In the following we omit the isospin (as well as spin) indices, since they are not relevant for the factorization we discuss. We also omit the $\vec{q}$ variables from the wave functions since by 3-momentum conservation (A3) they are fixed by $\vec{p}$ and $\vec{k}$. Thus we have

$$\begin{aligned} &V_A = V_A(\vec{p}_{C\perp} + \vec{p}_{D\perp}, P; \vec{k}_{A\perp}, x_A P),\\ &V_B = V_B(\vec{0}_\perp, P; \vec{k}_{B\perp}, x_B P),\\ &V_C = V_C(\vec{p}_{C\perp}, P; \vec{k}_{C\perp}, x_C P),\\ &V_D = V_D(\vec{p}_{D\perp}, P; \vec{k}_{D\perp}, x_D P). \end{aligned} \tag{A9}$$

Now, from Galilean invariance

$$\begin{aligned} &V_A = V_A(\vec{0}_\perp, P; \vec{k}_{A\perp} - x_A(\vec{p}_{C\perp} + \vec{p}_{D\perp}), x_A P),\\ &V_B = V_B(\vec{0}_\perp, P; \vec{k}_{B\perp}, x_B P),\\ &V_C = V_C(\vec{0}_\perp, P; \vec{k}_{C\perp} - x_C \vec{p}_{C\perp}, x_C P),\\ &V_D = V_D(\vec{0}_\perp, P; \vec{k}_{D\perp} - x_D \vec{p}_{D\perp}, x_D P). \end{aligned} \tag{A10}$$

It is clear that these wave functions must have a sharp falloff in transverse momenta. Therefore (if they fall off as $1/\vec{k}_\perp^{\,2}$ or faster) the main contribution to the integral comes from the regions where

$$\begin{aligned} &\vec{k}_{A\perp} \approx x_A(\vec{p}_{C\perp} + \vec{p}_{D\perp}), \quad \vec{q}_{A\perp} \approx (1 - x_A)(\vec{p}_{C\perp} + \vec{p}_{D\perp}),\\ &\vec{k}_{B\perp} \approx \vec{0}_\perp, \quad \vec{q}_{B\perp} \approx \vec{0}_\perp,\\ &\vec{k}_{C\perp} \approx x_C \vec{p}_{C\perp}, \quad \vec{q}_{B\perp} \approx (1 - x_C)\vec{p}_{C\perp},\\ &\vec{k}_{D\perp} \approx x_D \vec{p}_{D\perp}, \quad \vec{q}_{D\perp} \approx (1 - x_D)\vec{p}_{D\perp}. \end{aligned} \tag{A11}$$

This corresponds simply to the condition that the constituents carry a 2-momentum proportional to their x and the hadron momenta

$$\vec{k}_{i\perp} \approx x_i \vec{p}_{i\perp}, \quad (A12)$$

$$\vec{q}_{i\perp} \approx (1-x_i)\vec{p}_{i\perp}. \quad (A13)$$

As we discuss in more detail below, it is reasonable to assume that the wave functions favor small x_i. Therefore, the relation (A13) is in general more accurate than (A12). Therefore, to a good approximation we can set

$$\begin{aligned} C &= C(1-x_i, \vec{q}_{i\perp}) \\ &\approx C(1-x_i, (1-x_i)\vec{p}_{i\perp}) \\ &= C(1-x_i, (1-x_C)^2 t, (1-x_D)^2 u). \end{aligned} \quad (A14)$$

The last equality comes from using (A6) and (A11) and Galilean invariance. The entire dependence of C on the internal variables is through $1-x_i$. Thus one sees that the reliability of the approximations made in factorizing C outside the integral depends on (1) how peaked in x the wave functions are, and (2) how smooth C is in its dependence on $1-x_i$. The wave functions are related to the fractional longitudinal momentum distribution functions through

$$f(x) = \frac{1}{2(2\pi)^3} \int \frac{d^2\vec{k}_\perp}{x(1-x)} [V(\vec{0}, P; \vec{k}_\perp, xP)]^2. \quad (A15)$$

From lepton-proton scattering experiments we know that $f(x)$ falls off as $(1-x)^n$, where $n=3$ or 4 Near $x=0$ there is presumably a dip corresponding to a factor $x^{1-\alpha}$ with $\alpha \approx \frac{1}{2}$. Thus it is reasonable to assume that the major contribution to the integral comes from small x values, say, $x \approx 0.2$, which for a reasonably smooth C function motivates the approximate factorization.

---

*Work performed for the U. S. Energy Research and Development Administration under Contract No. W-7405-eng-82.

†Work supported by the Academy of Finland. Address until July 1976: University of California, Berkeley, California 94720.

[1]J. C. Doyle, F. S. Crawford, and J. A. Anderson, Phys. Rev. 165, 1483 (1968); T. O. Binford, M. L. Good, and R. R. Kofler, *ibid.* 183, 1148 (1969).

[2]N. A. Törnqvist, Nucl. Phys. B6, 187 (1968); Phys. Rev. 161, 1591 (1967).

[3]M. Korkea-aho and N. A. Törnqvist, Nucl. Phys. B33, 239 (1971); R. Ayed, P. Bareyre, and P. Sonderegger, Report No. 401 presented at the International Conference on High Energy Physics, Amsterdam, 1971 (unpublished); G. Höhler and W. Schmidt, Phys. Lett. 38B, 237 (1972); N. A. Törnqvist, Nucl. Phys. B64, 464 (1973); N. A. Törnqvist, Phys. Lett. 47B, 449 (1973).

[4]J. Ervanne, M. Korkea-aho, and N. A. Törnqvist, Physica Scripta 12, 305 (1975).

[5]M. G. Doncel, L. Michel, and P. Minnaert, Phys. Lett. 38B, 42 (1972).

[6]L. Michel, Nuovo Cimento 22, 203 (1961); R. J. N. Phillips, *ibid.* 26, 103 (1962); G. V. Dass, J. Frøjland, F. Halzen, Andre Martin, C. Michael, and S. M. Roy, Phys. Lett. 36B, 339 (1971); D. B. Ion and A. Mihul, Ann. Phys. (N.Y.) 92, 55 (1975); F. Kaiser, H. Kohl, and W. Schmidt, Lett. Nuovo Cimento 5, 413 (1972); N. W. Dean and W. F. Long, Phys. Rev. D 7, 3356 (1973).

[7]J. F. Gunion, S. J. Brodsky, and R. Blankenbecler, Phys. Rev. D 8, 287 (1973).

[8]S. Weinberg, Phys. Rev. 140, B516 (1965).

[9]J. B. Cheze *et al.*, Nucl. Phys. B72, 365 (1974).

[10]C. De Marzo *et al.*, Aix-en-Provence International Conference, 1973 (unpublished).

[11]R. P. Feynman, *Photon-Hadron Interactions* (Benjamin, Reading, Massachusetts, 1972); J. Kuti and V. F. Weisskopf, Phys. Rev. D 4, 3418 (1971).

[12]S. Weinberg, Phys. Rev. 150, 1313 (1966).